# Analysis of Terrace Width Distributions on Copper Vicinal Surfaces by a Wigner and a Gaussian Approach - A Comparison

M. Giesen[1] and T. L. Einstein[2]

[1] *Institut für Grenzflächenforschung und Vakuumphysik, Forschungszentrum Jülich, D 52425 Jülich, Germany*

[2] *Physics Department, University of Maryland, College Park, MD 20742-4111, USA*

**Abstract**

We have analyzed the terrace width distribution on Cu (100) and (111) vicinal surfaces using a standard Gaussian approximation as well as a previous developed Wigner approach based on random matrix theory. The Wigner approach provides reasonable results only for the case of asymmetric terrace width distributions. Then, both methods yield approximately the same results for the variances of the terrace width distributions. For approximately symmetric distributions where the Wigner approach should fail the Gaussian approximation provides good results.

## 1. Introduction

By examination of the *quantitatively measurable* terrace width distributions (TWD) on vicinal surfaces, one can extract information about the interaction between the steps. The typical analysis procedure makes use of the Gruber Mullins expression when there are no energetic interactions between the steps [1] and a similary-derived Gaussian approximation when these interactions are strong [2]. In a recent Letter, Einstein and Pierre-Louis observed that the so-called generalized Wigner surmise from random-matrix theory could describe these equilibrium fluctuations, as it does so many other fluctuation phenomena in physics [3]. This recognition relies on the mapping of the problem of interacting steps to that of the time evolution of fermions in one spatial dimension. The simple analytic expression provides an excellent approximation to the exact distribution for the three particular interactions for which the problem can actually be solved, as well as for other values in that range of interactions. That Letter offered a number of ideas on how to approach experimental data, but did not actually make contact with any. This Letter describes the first attempt to apply systematically this formula and viewpoint to a large number of closely related physical situations: both to nice ("typical") data and poor results, both to values within the range that the expression is expected to hold and to others beyond that range. We can thus assess which application procedures are viable and offer suggestions on how best to analyze data. The paper is organized as follows: In the second chapter, we describe the experimental set-up. We provide the reader with the essential theoretical ideas in chapter 3. This chapter is followed by the presentation and the discussion of the analysis of experimental results for various copper vicinal surfaces using both the standard Gaussian approximation and the generalized Wigner surmise.

## 2. Experimental

The experiments were performed in a standard ultra-high vacuum chamber with a base pressure of 5###$10^{-11}$ mbar. Our temperature variable scanning tunneling microscope (STM) is of the Besocke type. The experimental set-up and the sample cleaning are described in detail in previous publications [4, 5].

We used six different samples. Three of them were vicinal to the Cu (001) plane: Cu (117), (1 1 13) and (1 1 19). These crystal planes have miscut angles of 11.4°, 6.2° and 4.3° along the dense $[110]$-direction, respectively. The mean step separation is 8.9 Å (corresponding to 3.5 $a_\perp$, $a_\perp$ = 2.55 Å being the kink length), 16.6 Å ( 6.5 $a_\perp$) and 24.2 Å (9.5 $a_\perp$), respectively. The terraces are separated by parallel monatomic $[\bar{1}10]$-oriented steps. The other three surfaces are vicinals to the Cu (111) plane. Their miscut angles are 2.49°, 3.05° and 12.75° along the $[11\bar{2}]$-direction. These surfaces have an orientation (11 7 7), (19 17 17) and (23 21 21), respectively. The samples consist of parallel monatomic A-type steps along $[\bar{1}10]$. The mean terrace widths between adjacent steps are 10.2 Å (corresponding to 4.62 $a_\perp$, where $a_\perp$ = 2.21 Å is the kink length of a (100)-step on a (111)-surface), 32.3 Å (14.62 $a_\perp$) and 47.8 Å (21.63 $a_\perp$), respectively. The accuracy of the miscut angles for all surfaces is within 0.1°.

In our experiments, the concentration of pinning sites was lower than $10^{-7}$ per atom. For the analysis, we have chosen STM images obtained from areas free of residual contamination. A measured terrace width distribution was accepted for further analysis only when the average step density found from the distribution was consistent with the nominal step density given by the miscut angle of the surface. Fig. 1 shows STM images of (a) Cu (11 7 7) at 296 K and (b) Cu (23 21 21) at 303 K. The scan widths are 240 Å and 760 Å, respectively.

We used a computer code in order to determine the step-step distance distributions. This code searches for the maximum slope in a spline fitted to the gray scale values of each scan line perpendicular to the step edges. For each distribution we analyzed a total step length of 5-17 μm taken from 10-40 STM images from different areas of the sample.

**3. Theory**

In the downstairs direction on a vicinal surface, there is just one characteristic length, the average <L> of the spacings L. Hence, it is natural to plot the terrace width distribution (TWD) P(s) in terms of $s \equiv L/\langle L \rangle$. This distribution must be normalized, and by construction it has unit mean. In general there is a repulsion between the steps of the form $A/L^2$, due to elastic or dipolar forces, and there is always an entropic repulsion --because steps cannot cross--which obeys the same power-law decay. Then there are three energy-related quantities that characterize the problem: 1) the thermal energy, $k_B T$, which produces the fluctuations of the steps; 2) the stiffness of each step, $\tilde{\beta}$ [2], which opposes bending of the step and has units of energy per length[1]; 3) the strength A of the repulsion, which has units energy-length. There is only one dimensionless combination that can be formed: we define

$$\tilde{A} \equiv \frac{A\tilde{\beta}}{(k_B T)^2} \qquad (1)$$

[1] Equivalently, $\tilde{\beta}$ can be written as $\frac{k_B T\, a_{\parallel}}{b^2}$, where $b^2$ is the diffusivity [2] and $a_{\parallel}$ the lattice spacing along the step. The diffusivity can be expressed in terms of the kink formation energy $\varepsilon$

Since steps do not start, end, or cross, the set of their configurations is equivalent to world lines of free fermions evolving in one spatial dimension (i.e. (x,t) plots). When A=0, these are free fermions. The venerable Gruber -Mullins approximation fixes the two neighboring steps of an (active) step to be straight and separated by twice the average spacing [1]. By analogy to the problem of a particle in a 1-D box, it is easy to show

$$P(s) = \sin^2\left(\frac{\pi\, s}{2}\right) \qquad (2)$$

Analytic approximants containing large numbers of elementary functions provide an arbitrarily accurate representation of the exact result [7], but can be inconvenient to use. When there are strong repulsions between the steps, so that the motion of each step tends to be confined near its mean position, a Gruber-Mullins argument shows that P(s) can be approximated by a Gaussian [1, 2]

$$P(s) = \frac{1}{\sigma\sqrt{2\pi}}\, e^{\frac{(s-1)^2}{2\sigma^2}} \qquad (3)$$

where the width

---

assuming that the energy of kinks is proportional to the kink length [6]:

$$b^2 = \frac{2}{\exp\left(-\frac{\varepsilon}{k_B T}\right) + \exp\left(\frac{\varepsilon}{k_B T}\right) - 2}$$

$$\sigma = \frac{1}{\left(48\,\tilde{A}_G\right)^{1/4}}, \tag{4}$$

if only nearest neighbors are considered and

$$\sigma = \left(\frac{15}{8\,\pi^4\,\tilde{A}_G}\right)^{1/4} \tag{5}$$

if all steps are included. (Since the coefficient of $\tilde{A}_G$ in the latter is about 8% larger, the estimate of $\tilde{A}_G$ is about that much smaller than that deduced assuming just nearest-neighbor interactions.)

Most of the above is well known, as is the fact that for $\tilde{A}$ = 2, 0, and -1/4, exact solutions exist [8]. The new idea is that random-matrix theory [9, 10] teaches that fluctuations should have a universal form determined by the symmetry of the couplings of the states. The so-called generalized Wigner surmise proposes that one can approximate [3]

$$P_\rho(s) = a_\rho\, s^\rho\, \exp\left(-b_\rho\, s^2\right), \tag{6}$$

where the exponent $\rho$ is related to $\tilde{A}_W$ (via the Sutherland Hamiltonian [8]) by

$$\rho = 1 + \sqrt{1 + 4\,\tilde{A}_W}\ . \tag{7}$$

The constants $a_\rho$ and $b_\rho$ are determined by the two conditions of normalization and unit mean. This formula represents an interpolation scheme between the values 1, 2, and 4 for $\rho$ (or -1/2, 0, and 2 for $\tilde{A}_W$) for which the exact solutions occur. At these three calibration points, the Wigner expressions $P_1$, $P_2$ and $P_4$ provide remarkably accurate -- while still simple -- approximations of the corresponding exact distributions, within a couple percent. For values well beyond $\rho$ = 4, there is no reason to expect the Wigner form to provide a better approximation than the Gaussian one, and several reasons to doubt it.

Given the simple analytic form of the Wigner distribution, it is straightforward to deduce a number of statistical properties. We first note the explicit values of the two $\rho$-dependent constants $a_\rho$ and $b_\rho$ [3] :

$$b_\rho = \left[\frac{\Gamma\left(\frac{\rho+2}{2}\right)}{\Gamma\left(\frac{\rho+1}{2}\right)}\right]^2 \quad \text{and} \quad a_\rho = \frac{2\,b_\rho^{(\rho+1)/2}}{\Gamma\left(\frac{\rho+1}{2}\right)} \tag{8}$$

These two constants turn out to be rather linear in $\rho$, so that in trying to deduce the value of $\rho$ from data, it may be convenient to use expansions, e.g. about $\rho$ = 4:

$$\begin{aligned} b_\rho &\approx 2.2635 + 0.4971(\rho-4) + 0.0006(\rho-4)^2 + O[\rho-4]^3 \\ \ln a_\rho &\approx 2.4508 + 0.6060(\rho-4) - 0.0111(\rho-4)^2 \\ &\quad + 0.0015(\rho-4)^3 - 0.0002(\rho-4)^4 + O[\rho-4]^5 \end{aligned} \tag{9}$$

Eq. (7) provides an excellent approximation for the constants $a_\rho$ and $b_\rho$ for $2 \le \rho \le 6$. In dealing with data, it is more convenient to compute moments of the order n about the origin than about the mean [3]:

$$\mu_n' = \int_0^\infty s^n P(s)\, ds \qquad (10)$$

Specifically, the second moment $\mu_2'$, i.e.

$$\mu_2' = 1 + \sigma_w^2 \ , \qquad (11)$$

(where the variance $\sigma$ is the typically-measured feature of the TWD) is

$$\mu_2' = \frac{\rho + 1}{2 b_\rho} \qquad (12)$$

A distinctive feature of Gruber-Mullins approximations [1] is that the distribution is symmetric about the mean. While this approximation is not bad for strong repulsions, it obviously is not good as one approaches the free-fermion limit. The standard way to describe the asymmetry is to compute the skewness, defined in terms of the third moment about the mean as [3]

$$\frac{\mu_3' - 1}{\sigma^3} - \frac{3}{\sigma} \quad \text{where} \quad \mu_3' = \frac{\rho + 2}{2 b_\rho} \ . \qquad (13)$$

Since A is relatively independent of T while $\tilde{\beta}$ decreases with it (weakly, until the roughening transition is approached), $\tilde{A}$ decreases strongly with T. Thus, looking at the same sample at several different temperatures provides a scan in $\tilde{A}$, even though not in A.

Ref. [3] suggested that a fruitful way to determine $\rho$ or $\tilde{A}$ is to fit separately the second and the third moments of the distribution. This proposal turns out not to work well with actual data. The moments are too sensitive to the errors in the measured distribution and the discreteness of the possible terrace widths.

**4. Results**

Fig. 2 shows terrace width distributions (TWD) measured on a Cu (1 1 13) surface at different temperatures. The experimental data is plotted as open circles. The experimental distributions are normalized with respect to the experimentally determined mean terrace widths in each specific measurement. We also analyzed the TWD using the nominal mean terrace width given by the miscut angle. It turns out that the Wigner analysis depends sensitively on the scaling factor. Differences between the nominal value and the experimentally determined mean terrace width of less than half an atom introduce large errors to the analysis. With respect to a simple determination of the variance of the distribution, the Gaussian analysis is less sensitive to deviations of the mean value from the nominal terrace width. Here, deviations of the order of half an atom still provide good results.

For low temperatures, the experimental distribution is approximately symmetric. Here, both the Wigner (solid curve) and the Gaussian (dashed curve) model provide excellent fits to the data. At low temperatures the value of $\rho$ determined using the Wigner surmise is relatively large ($\rho$ = 7.5 at 295 K). With increasing temperature, the asymmetry of the step-step distance distribution increases and the value of $\rho$

decreases ( $\rho$ = 4.7 at 348 K). Though the Gaussian distribution still is in reasonable agreement with the data in the vicinity of the distribution peak it fails in the range of large step separations. On the other hand, the Wigner expression gives a slightly less accurate accounting in the range of the distribution peak, though it reasonably fits the range of large step-step distances.

In Fig. 3 two distributions measured for copper (111) vicinal surfaces are shown. For comparison we have chosen one distribution measured for the (11 7 7) plane in equilibrium and one for the (19 17 17) plane where the TWD is obviously not in equilibrium. The data corresponding to (19 17 17) displays a double-peak distribution. In addition we also show the variances using eqs. (11,12) and the variance obtained from the Gaussian fit, respectively, in both panels in Fig. 3. Whereas in the top panel the Wigner as well as the Gaussian model provide good agreement with the experimental data, the data in the lower panel is obviously not fitted by either of the models. The variances determined using the two models in the first case agree well: their difference is less than 4 %. This deviation is much less than that due to typical experimental errors. Errors are introduced e.g. by slight deviations of the experimental distribution from the true equilibrium distribution. Except for obvious cases like shown in the lower panel of Fig. 3, deviations of this nature must be anticipated.

Table 1 gives an overview of representative data obtained by analyzing TWDs measured on various copper vicinal surfaces as a function of the temperature. For the Cu (1 1 13) surface it is shown in Fig. 2 that the TWD becomes broader and more asymmetric for increasing temperature. This is reflected in table 1 by a decreasing value of $\rho$ for increasing temperature, as is expected from eq.(1) and subsequent discussion. We obtain values of $\rho$ between 3.5 and 8.6. For low temperatures, the interaction potential on copper is strongly repulsive corresponding to $\rho$ well above 4.

In our experiments, the distribution becomes slightly asymmetric, though far from the free fermion limit, in the high-temperature range.

Columns 3 to 6 in table 1 show the interaction constants $\tilde{A}_W$ (eq.(7)), $\tilde{A}_G$ (eq.(5)) and $A_W$, $A_G$ (eq.(1)) for the Wigner and the Gaussian fit, respectively. While the constants $\tilde{A}_W$ and $\tilde{A}_G$ are dimensionless, the interaction constants $A_W$, $A_G$ are given in meV $\cdot \frac{a_\perp^2}{a_\parallel}$. For $\rho$ of the order of 5 and smaller, the results obtained using both models are in excellent agreement. It is shown in particular that the additional factor of about 3 proposed by Ihle et al. [11] and Masson at al. [12] is not correct. For larger values of $\rho$, the Wigner model overestimates the interaction constant by about a factor of 1.5 - 2. The overestimation is expected from the theory discussed in ref. [3]. The good agreement between the interaction constants determined by the Wigner and the Gaussian model becomes obvious from all measurements that we performed. The error bars for $A_W$ are generally larger than for $A_G$. This is probably to the fact that the Wigner surmise sensitively depends on the distribution values at larger step-step distances. In this range, however, the statistical data base is lower than for the range around the distribution peak. Therefore, the experimental distributions with large asymmetry generally display a higher noise level for large step-step distances which again introduces a larger scattering in the determination of $\rho$ in the Wigner surmise.

In column 7 we have tabulated the values for $T^2\ \tilde{A}_W$ in units of $10^6$ $K^2$. As is proposed by eq.(1), this quantity obeys the same temperature dependence than the step edge stiffness $\tilde{\beta}$. Fig. 4 shows $T^2\ \tilde{A}_W$ for the complete data set obtained for Cu (1 1 13). The open circles are the experimental data and the solid curve is the theoretical prediction using eq.(1) and a kink formation energy of $\varepsilon$ = 0.128 meV [13,

14]. Concerning the error bars introduced by the error of $\tilde{A}_W$ given in table 1, the experimental data is in agreement with the theoretical prediction.

In our experiments, we find no values of $\rho$ smaller than 3.5. Here, the Gaussian fit still provides comparable results to the Wigner surmise. For lower values of $\rho$, the Gaussian model is expected to fail. In order to reach this limit, one would have to measure step-step distance distributions at higher temperatures than shown here. For this purpose, however, one would need samples with a larger mean step-step separation: With increasing temperature, the equilibrium fluctuations of steps increase. When the mean amplitude of these fluctuations are of the order of half the step separation, it becomes difficult (if not impossible) to distinguish positions of adjacent steps. For the measurements on copper surfaces presented here, temperatures up to 370 K are the upper limit for the determination of step positions. When using samples with lower step densities, however, one is restricted by residual pinning sites at step edges. The influence of residual pinning sites on the TWD becomes more important for larger mean step separations. Hence, it becomes more difficult to measure equilibrium distributions.

Although the Wigner surmise is expected to provide good agreement with the Gaussian fit only for $\rho$ less than about 6, the variances $\sigma^W_{theory}$ (eq.(11)) and $\sigma^G_{exp}$ determined from the Gaussian fit are in excellent agreement for all values of $\rho$ up to 8.6 measured in our experiments. This is in particular the case also when the peak of the Gaussian is not exactly posited at s=1 due to noise in the experimental data in the peak area. That is, the determination of the variance using a Gaussian fit is very reliable also for shifted and slightly asymmetric distributions. Hence, the Gaussian analysis also provides excellent results for the variances and the interaction constants when an experimental distribution is not normalized with respect to the

mean terrace width and unit mean, and so is more forgiving than the Wigner approach.

We have also determined the second and the third moment of the experimental distributions (eq. (10)) The experimentally determined second moment around the origin $\mu_2'(\text{exp})$ (eq.(10)) is given in column 7 of table 1. For comparison we have tabulated the theoretically expected value $\mu_2'(\text{theory})$ (eq.(12)) in column 8. As though the experimentally and theoretically determined values are partially in good and partially in reasonable agreement, the deviation of $\mu_2'(\text{exp})$ from $\mu_2'(\text{theory})$ is significant. For the case of Cu (1 1 13) at 320K the value of $\rho$ determined from the experimental second moment would be 4.5 rather than 5.2. The scattering in the results for the second moment is due to noise in the experimental data. Even for a very large data base like used in our experiments, the evaluation of $\mu_2'(\text{exp})$ sensitively depends on the noise of the data. Hence, the determination of the second moment from an experimental distribution is not a reliable method to obtain information about $\rho$ and the step-step interaction. The influence of noise in the experimental data becomes even more dramatic for the determination of the third moment and hence the skewness (eq. (13)). Here, the results obtained may also become negative. Therefore, we have not listed the third moments in table 1.

**5. Summary**

In summary we have demonstrated that the results obtained from an analysis of the TWD on copper vicinal surfaces using the generalized Wigner surmise is in good agreement with those obtained from the standard Gaussian analysis for slightly asymmetric distributions. In particular, we have shown that the standard Gaussian analysis based on the hard-wall model proposed by Bartelt and coworkers has to be applicated in order to analyze TWDs. The Gaussian analysis proposed by Ihle et al.

and Masson et al. introducing an additional factor of about 3 considering the motion of a single step between immobile neighboring steps provides no correct results. We have also demonstrated that the determination of the moments of TWDs generally offers no reliable information on experimental TWDs due to large errors caused by noise in the experimental data.

**Acknowledgement**

The authors thank for the skillful sample preparation by U. Linke. Helpful contributions concerning the computer codes for the determination of the step positions in the STM images by H. Ibach are gratefully acknowledged. TLE further appreciates the support of a Humboldt U.S. Senior Scientist Award.

???

**References:**

[1] E. E. Gruber, W. W. Mullins, J. Phys. Chem. Solids 28 (1967) 875.

[2] N. C. Bartelt, T. L. Einstein, E. D. Williams, Surf. Sci. 240 (1990) L591.

[3] T. L. Einstein, O. Pierre-Louis, submitted to Phys. Rev. Lett. (1998) .

[4] M. Giesen, Surf. Sci. 370 (1997) 55.

[5] M. Giesen, G. S. Icking-Konert, Surf. Rev. Lett., in press (1998) .

[6] M. Poensgen, J. F. Wolf, J. Frohn, M. Giesen, H. Ibach, Surf. Sci. 274 (1992) 430.

[7] B. Joós, T. L. Einstein, N. C. Bartelt, Phys. Rev. B43 (1991) 8153.

[8] B. Sutherland, Journal of Mathematical Physics 12 (1971) 246.

[9] M. L. Mehta, *Random Matrices*, Academic, New York 1991.

[10] T. Guhr, A. Müller-Groeling, H. A. Weidmüller, Phys. Rep. submitted (1998) .

[11] T. Ihle, C. Misbah, O. Pierre-Louis, Phys. Rev. B 58 (1998) 2289.

[12] L. Masson, L. Barbier, J. Cousty, Surf. Sci. 317 (1994) L1115.

[13] M. Giesen-Seibert, H. Ibach, Surf. Sci. 316 (1994) 205.

[14] M. Giesen-Seibert, F. Schmitz, R. Jentjens, H. Ibach, Surf. Sci. 329 (1995) 47.

**Figure Captions:**

**Fig. 1:** STM images of (a) Cu (11 7 7) at T = 296 K and (b) Cu (23 21 21) at T= 303 K. The scan widths are 240 and 760 Å, respectively. The monatomic steps run from top to bottom and the surface height increases from left to right.

**Fig. 2:** TWD measured for Cu (1 1 13) at different temperatures. The solid curves are fits using the Wigner approach (eq. (6). The dashed curves are fits to a Gaussian.

**Fig. 3:** TWD measured for two Cu (111) vicinal surfaces. The upper panel shows "typical" data, whereas the lower shows "poor" data. The solid and dashed curves are fits to the data using the Wigner and the Gaussian approach, respectively.

**Fig. 4:** Temperature dependence of $T^2\ \tilde{A}_W$ (open circles). The solid curve is a theoretical curve calculated using eq. (1).

| Surface | T | $\rho$ | $\tilde{A}_W$ | $\tilde{A}_G$ | $\tilde{A}_{Pl}$ | $A_W$ | $A_G$ | $A_{Pl}$ | $T^2\tilde{A}_W$ | $\mu_2'$(exp) | $\mu_2'$(theory) | $\mu_3/\sigma^3\|_{Pl}$ | $\sigma^W_{exp}$ | $\sigma^W_{theory}$ | $\sigma^G_{exp}$ |
|---|---|---|---|---|---|---|---|---|---|---|---|---|---|---|---|
| ***Cu (1,1,7)*** | 298 | $8.6 \pm 0.5$ | 14.3 | 10.1 | 26.9 | $5.1 \pm 0.8$ | 3.6 | 19.6 | 1.27 | 1.045 | 1.055 | 0.209 | 0.213 | 0.234 | 0.209 |
| ***Cu (1,1,13)*** | 295 | $7.5 \pm 0.3$ | 10.3 | 5.3 | 11.5 | $3.4 \pm 0.3$ | 1.7 | 3.8 | 0.90 | 1.062 | 1.061 | 0.252 | 0.249 | 0.247 | 0.246 |
| | 320 | $5.2 \pm 0.5$ | 4.1 | 3.9 | 5.5 | $2.2 \pm 0.6$ | 2.1 | 3.0 | 0.42 | 1.111 | 1.084 | 0.293 | 0.334 | 0.289 | 0.265 |
| | 348 | $4.7 \pm 0.4$ | 3.1 | 3.5 | 4.4 | $2.7 \pm 0.7$ | 2.9 | 3.8 | 0.38 | 1.183 | 1.092 | 0.307 | 0.428 | 0.303 | 0.273 |
| ***Cu (1,1,19)*** | 320 | $6.4 \pm 0.4$ | 7.1 | 3.8 | 7.8 | $3.9 \pm 0.5$ | 2.0 | 4.2 | 0.73 | 1.179 | 1.070 | 0.274 | 0.423 | 0.264 | 0.267 |
| | 370 | $4.5 \pm 0.7$ | 2.1 | 2.3 | 2.5 | $2.5 \pm 1.4$ | 2.7 | 3.0 | 0.29 | 1.099 | 1.103 | 0.340 | 0.315 | 0.322 | 0.302 |
| ***Cu (11,7,7)*** | 296 | $5.5 \pm 0.7$ | 4.8 | 4.5 | 6.4 | $3.3 \pm 1.2$ | 3.3 | 4.5 | 0.42 | 1.034 | 1.080 | 0.285 | 0.186 | 0.283 | 0.252 |
| | 306 | $4.6 \pm 0.5$ | 3.0 | 3.6 | 6.7 | $2.5 \pm 0.9$ | 2.9 | 3.7 | 0.28 | 1.079 | 1.092 | 0.282 | 0.281 | 0.304 | 0.270 |
| ***Cu (19,17,17)*** | 333 | $3.5 \pm 0.3$ | 1.3 | 1.7 | 1.1 | $1.6 \pm 0.5$ | 2.1 | 1.4 | 0.14 | 1.166 | 1.118 | 0.389 | 0.407 | 0.343 | 0.328 |
| | 353 | $4.0 \pm 0.3$ | 2.1 | 2.1 | 2.2 | $3.5 \pm 0.8$ | 3.4 | 3.7 | 0.26 | 1.094 | 1.104 | 0.349 | 0.306 | 0.322 | 0.311 |
| ***Cu (23,21,21)*** | 328 | $5.3 \pm 0.3$ | 4.5 | 2.9 | 5.2 | $5.4 \pm 0.7$ | 3.3 | 6.2 | 0.48 | 1.082 | 1.082 | 0.297 | 0.286 | 0.286 | 0.286 |

**Table I:**

Value of $\rho$ determined from a Wigner fit (eq. (6)) for various copper surfaces at different temperatures. The temperature is given in K and $\rho$ is a dimensionless number. In addition, the values for $\tilde{A}_W$ (eq.(7)) $\tilde{A}_G$ (eq.(5)) and $\tilde{A}_{Pl}$ (eq.(?)) determined from the Wigner fit, the Gaussian fit and the approach suggested by Plummer are given. The interaction constants $A_W$, $A_G$ and $A_{Pl}$ are given in units of meV $\cdot \frac{a_\perp^2}{a_\parallel}$, where $a_\perp = 0.221\,\text{nm}$ and $a_\parallel = 0.255\,\text{nm}$ for the Cu(111) vicinal surfaces and $a_\perp = a_\parallel = 0.255\,\text{nm}$ for the Cu(100) vicinal surfaces. The temperature dependence of $T^2\,\tilde{A}_W$ is that of the step edge stiffness $\tilde{\beta}$ (eq.(1)) and is given in $10^6$ K$^2$. $\mu_2'$(exp) is the second moment over the origin determined from the experimental terrace width distribution (eq.(10)). $\mu_2'$(theory) is the theoretically expected value of the second moment over the origin using the experimentally determined value of $\rho$ and eq.(12). $\mu_3/\sigma^3|_{Pl}$ is the skewness, determined following the approach suggested by Plummer (eq. (?)). $\sigma^W_{exp}$ and $\sigma^W_{theory}$ are the variances calculated from $\mu_2'$(exp) and $\mu_2'$(theory), respectively, using eq.(11). $\sigma^G_{exp}$ is the variance determined from a Gaussian fit to the experimental terrace width distributions.

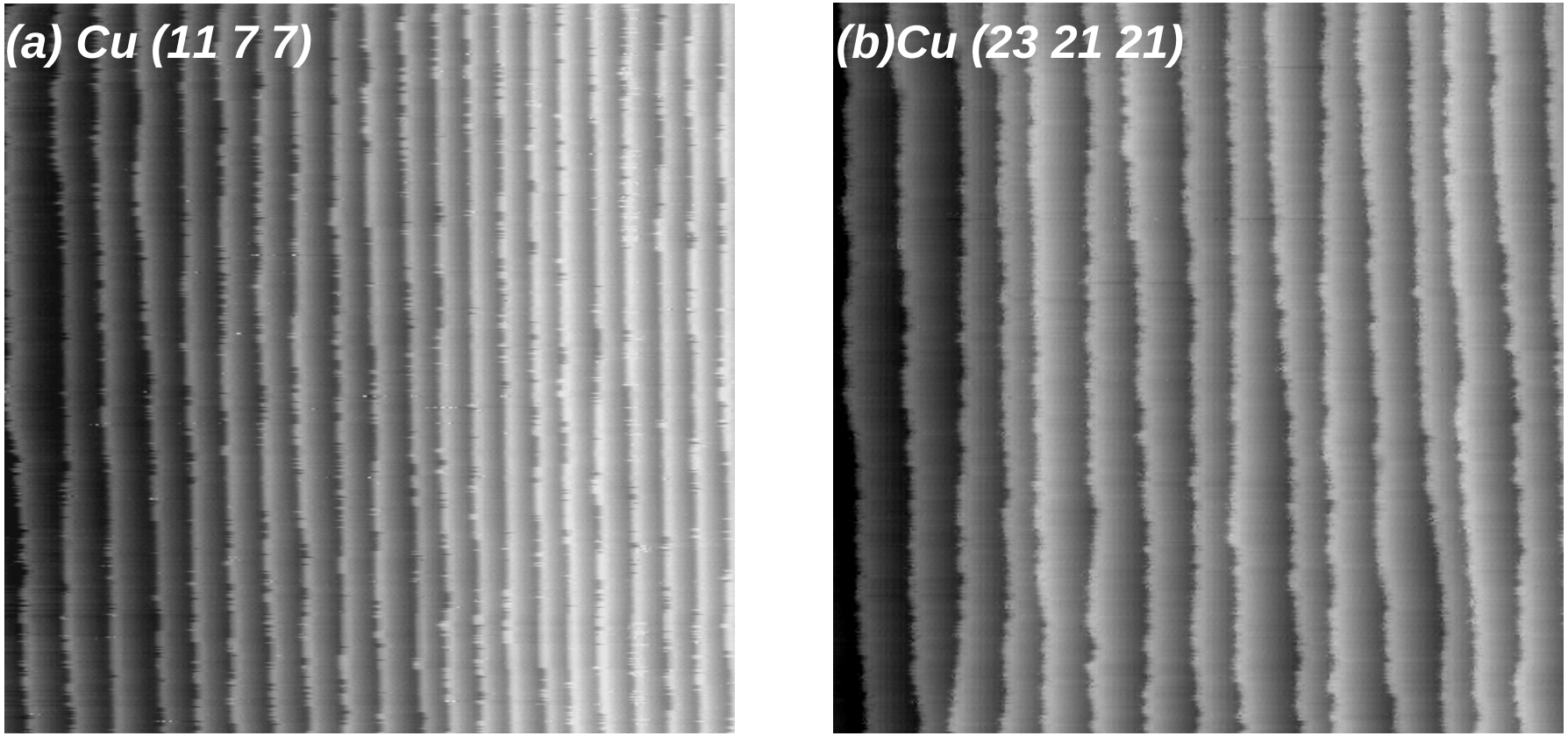


**Fig. 1**

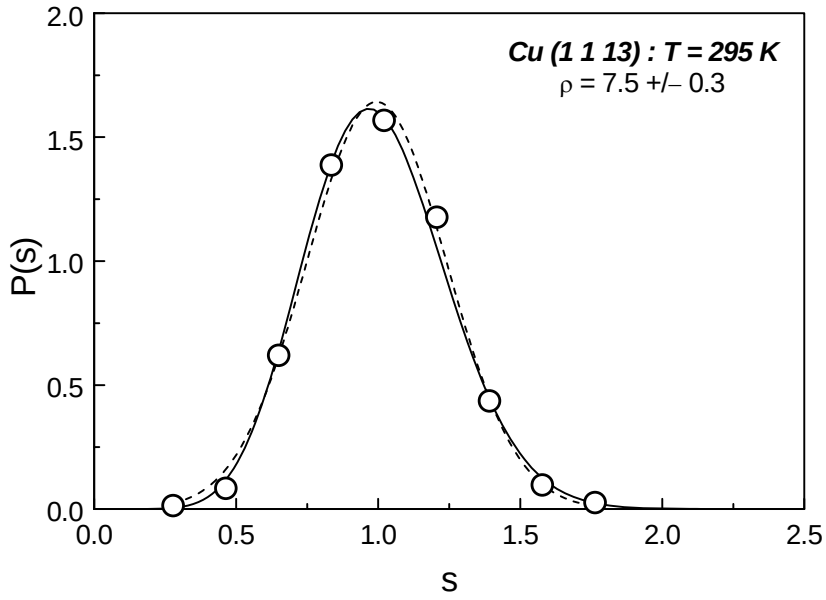
Cu (1 1 13) : T = 295 K
ρ = 7.5 +/– 0.3
P(s)
s
0.0
0.5
1.0
1.5
2.0
2.5

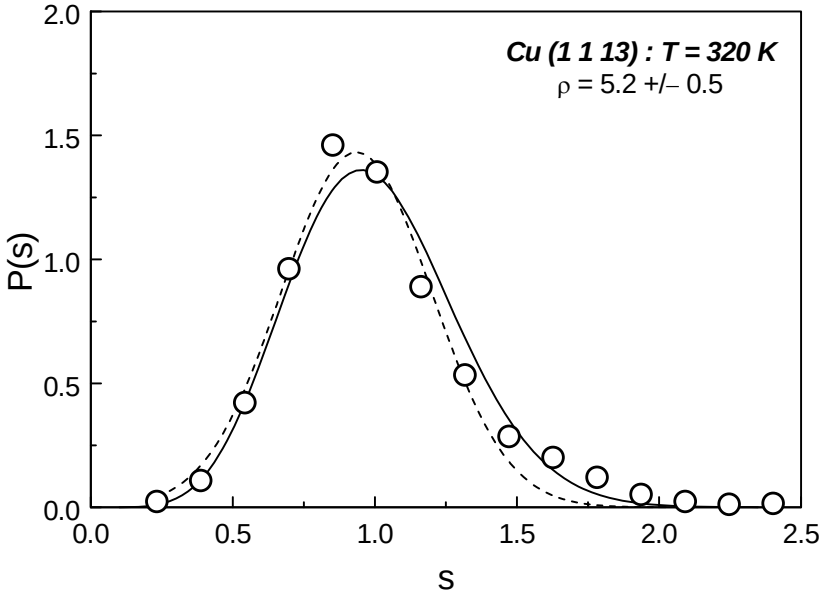
Cu (1 1 13) : T = 320 K
ρ = 5.2 +/– 0.5
P(s)
s
0.0
0.5
1.0
1.5
2.0
2.5

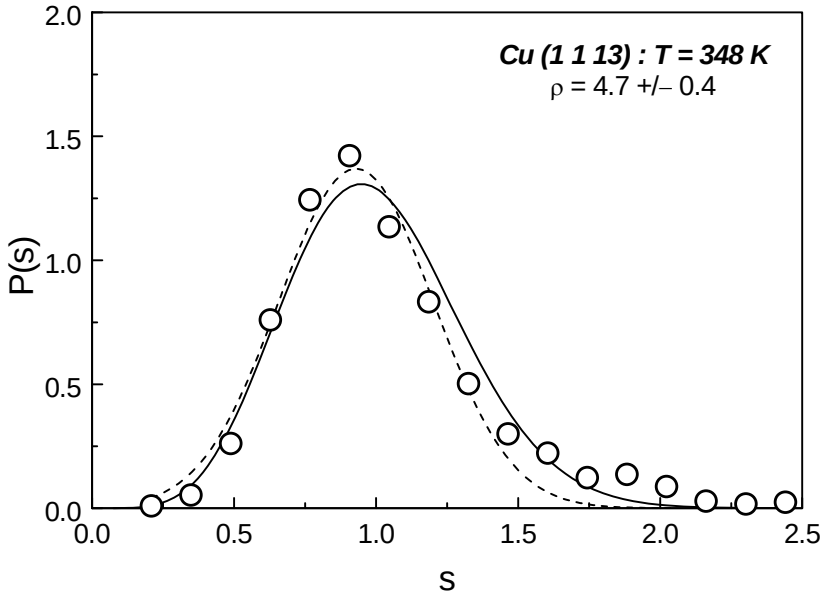
Cu (1 1 13) : T = 348 K
ρ = 4.7 +/– 0.4
P(s)
s
0.0
0.5
1.0
1.5
2.0
2.5

**Fig. 2**

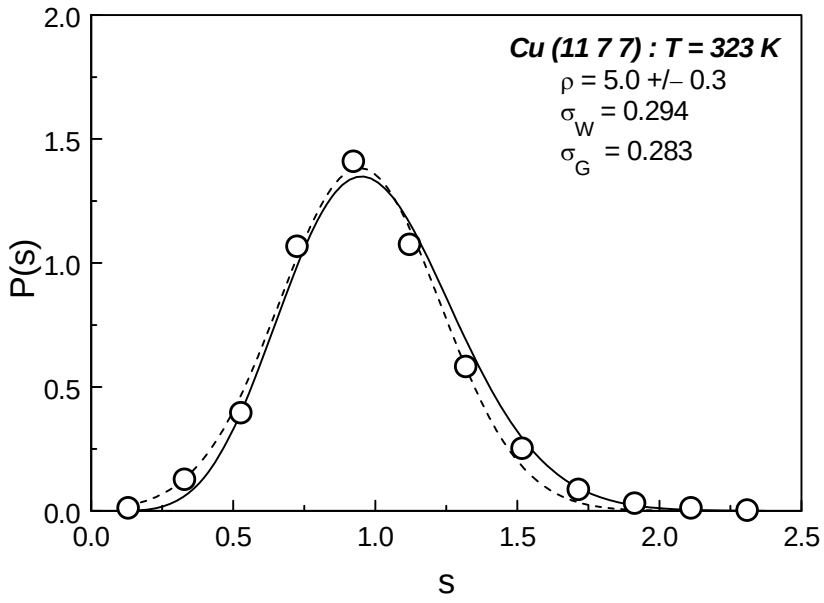
Cu (11 7 7) : T = 323 K
ρ = 5.0 +/– 0.3
σW = 0.294
σG = 0.283
P(s)
s
0.0
0.5
1.0
1.5
2.0
2.5

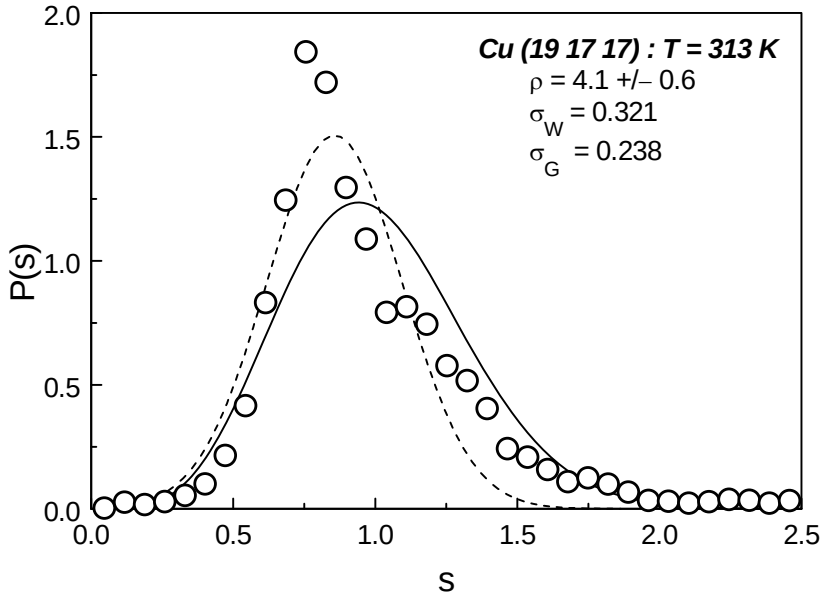
Cu (19 17 17) : T = 313 K
ρ = 4.1 +/– 0.6
σW = 0.321
σG = 0.238
P(s)
s
0.0
0.5
1.0
1.5
2.0
2.5

**Fig. 3**

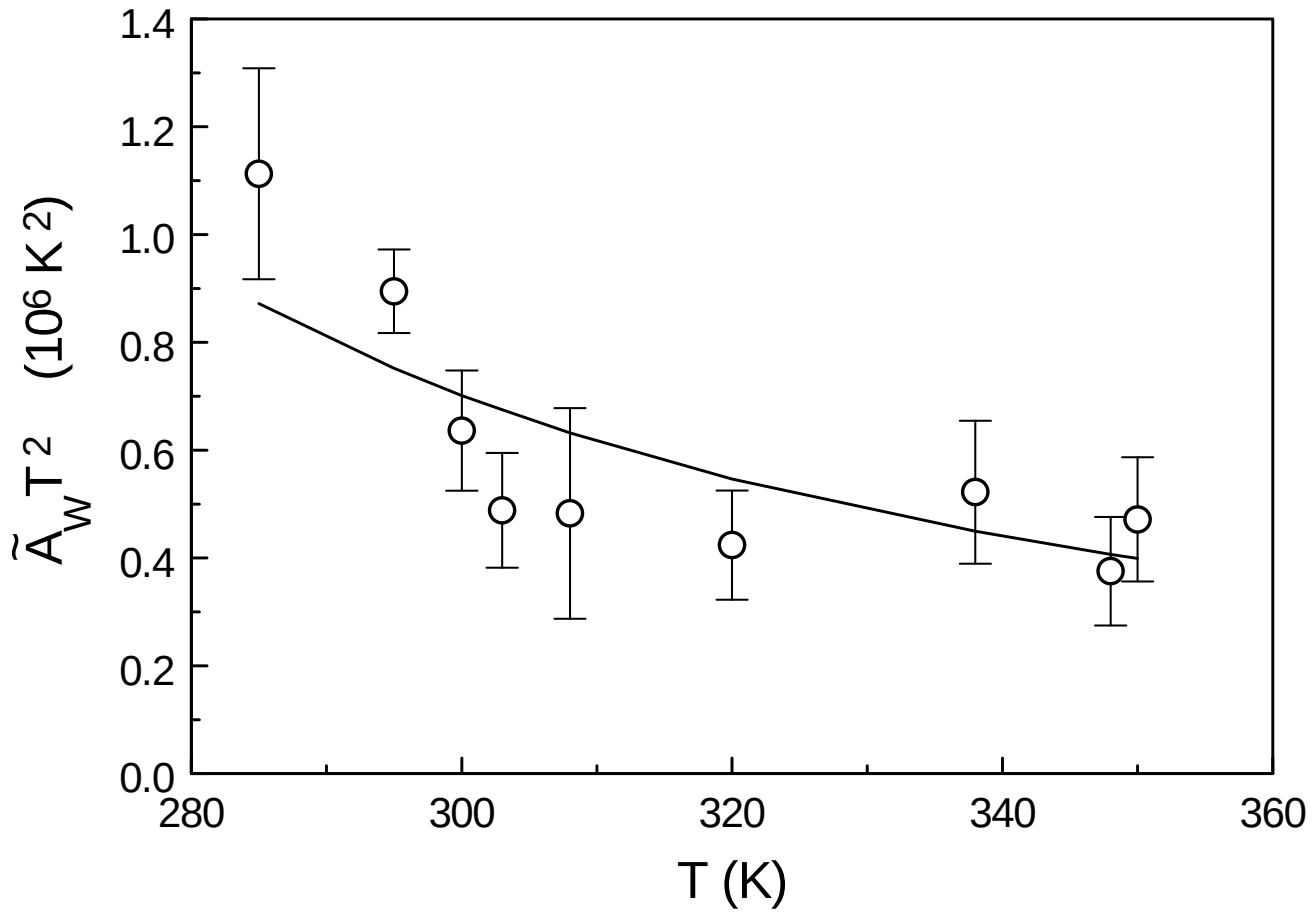


**Fig. 4**